

Research Article

Photovoltaic Performance Improvement of Dilute Nitrides GaAs_{1-x}N_x-Based Thin-Film Solar Cell Structure Using SCAPS-1D Software

Zamil Sultan* , Nuralam Howlader , Forhad Hossen , Asaduzzaman Joy ,
Asadul Haque

Department of Electrical and Electronic Engineering, Hajee Mohammad Danesh Science and Technology University, Dinajpur, Bangladesh

Abstract

The recent industrial revolution has increased the demand for the possible use of renewable energy sources to meet the World's high energy requirements and to minimize the quantity of green-house gases (GHGs) in the atmosphere at once in a sustainable manner. Solar energy is one of the renewable energy sources that has garnered the most attention for sustainable energy production because it is ecologically benign, clean as well as widely available. The main issue with solar cells in comparison to traditional systems, however, continue to be their greater cost and efficiency restriction. It is anticipated that the issues will be resolved as the technology progresses as well as precious fabricating materials are used more. Dilute nitrides compound semiconductors, such as GaAs_{1-x}N_x, GaP_{1-x}N_x and Ga_yIn_{1-y}As_{1-x}N_x have become promising materials because they have unique properties suitable for novel next generation optoelectronics especially photovoltaic applications. In addition, among dilute nitrides, GaAs_{1-x}N_x attracts much attention to the researchers because of its excellent absorption coefficients and charge-transport properties, which are importantly desirable for high efficiency solar cell. Therefore, in this research work, the thin-film solar cell's performance metrics with dilute nitrides GaAs_{1-x}N_x as absorber layer were investigated by SCAPS-1D. The impacts of bandgap bowing and absorber layer's thickness as well as operating temperatures, work functions of back-contact were evaluated to optimize open-circuited voltage (V_{oc}), short-circuited current density (J_{sc}), fill-factor (FF) and efficiency (η). The absorber layer's bandgap dependence performances study revealed that efficiency around 46% can be achieved with exceptional feasibilities such as lower density of as-grown defects and reliable lifetime by tuning bandgap to 0.82eV via adjusting nitrogen concentration in GaAs_{1-x}N_x. The assessment of performance for different absorber layer thicknesses showed that thickness around 2000nm is ideal for improving the suggested solar cell efficiency. Furthermore, higher efficiency and optimized other performance parameters obtaining at temperature 300K suggested that it is preferable to run the solar cell at that temperature to ensure steady-state functioning. Finally, it was explored by evaluating dependence of V_{oc} , J_{sc} , FF and η on back-contact work functions at two bandgap energies of absorber layer that specially J_{sc} was dramatically influenced with changing bandgap of absorber layer. The research findings would be helpful for emerging renewable energy-based nanotechnology for reducing the world higher energy crisis and green-house gases at once in a sustainable manner.

Keywords

Thin-Film Solar Cell, Dilute Nitrides Semiconductors, Solar Energy, Fill-Factor, Efficiency, Short-circuited Current Density

*Corresponding author: mdzamilsultan@hstu.ac.bd (Zamil Sultan)

Received: 8 October 2024; Accepted: 12 November 2024; Published: 29 November 2024



Copyright: © The Author(s), 2024. Published by Science Publishing Group. This is an **Open Access** article, distributed under the terms of the Creative Commons Attribution 4.0 License (<http://creativecommons.org/licenses/by/4.0/>), which permits unrestricted use, distribution and reproduction in any medium, provided the original work is properly cited.

1. Introduction

Currently, the demand of energy increases day by day for technological and industrial development worldwide even though there is a finite supply of fossil fuels like coal, natural gas and oil etc. Furthermore, the continuous rise in the quantity of carbon dioxide (CO₂) and other greenhouse gases (GHGs) in the atmosphere by energy combustion and industrial operations is a severe global warning to everyone regarding climate change in the recent year [1, 2]. In these circumstances, renewable, green and clean energy sources have attracted significant attention because of their potential use can fulfill global high energy requirements [3-5] as well as minimize the concentration of GHGs in the atmosphere simultaneously and sustainably. Amongst renewable energy sources, solar energy is considered highly significant renewable and sustainable source for energy production [6] for being environmentally friendly as well as huge globally. However, the main issues of solar cells in contrast to traditional systems are still their comparatively higher cost [7] and efficiency limitations. The problems are expected to be overcome as the technology progresses. For single junction photovoltaic cells, a band gap greater than 1.7 eV is not conducive so using a relatively wide band gap is common [8]. The maximum efficiency limit is found to be as 33.7% for a single junction solar cell based on the Shockley-Queisser (S-Q) numerical calculations [9]. A strategy utilizing the multi-junction solar cells was investigated to get around the drawbacks of single junction solar cell [10]. By stacking several semiconductor layers with the topmost layer having the peak energy band gap, photons with different energies of the solar spectrum can be absorbed by the different layers allowing higher light conversion efficiencies which exceed the theoretical S-Q limit. Nevertheless, the structure has structural complexity issue. A thin-film solar cell is a more modest option in terms of cost/watt ratio [11], light weight [12] and adaptable manufacturing technique [13]. Since the basic performance metrics of solar cells including open circuit voltage (V_{oc}), short circuit current density (J_{sc}), fill-factor (FF) and efficiency (η) can be accurately regulated by fabrication materials as well as physical configurations, a significant amount of research may be done on this device to improve its performance by fine-tuning its structure, structural parameters and fabrication materials.

In the recent years, dilute nitrides semiconductors, such as GaAs_{1-x}N_x, GaP_{1-x}N_x and Ga_yIn_{1-y}As_{1-x}N_x which are members of group III-V compound semiconductors have become promising materials because they have unique properties suitable for novel next generation optoelectronics [14, 15], especially photovoltaic applications [16]. Previous studies on dilute nitrides revealed that large band-gap bowing is occurred in these alloys by incorporating a few percentage of nitrogen into these alloys [17-19] which makes it possible or feasible of tuning band gap energy within the range of solar

energy spectrum. In addition, among dilute nitrides, GaAs_{1-x}N_x attracts much attention to the researchers because of its excellent absorption coefficients and charge-transport properties [3], which are importantly desirable for high efficiency solar cell. Previous study on GaAsN alloy also revealed that the photoluminescence (PL) intensity improvement occurs in this alloy during laser irradiation [20] which is an evidence of the reliability and longer life-time during operation. Because of these superior properties, GaAs_{1-x}N_x with different nitrogen concentrations has been considered as an absorber layer of thin film solar cell in this study for optimizing solar cell performances. In addition, n-GaAs has been used as a buffer or window layer in this study. GaAs devices are less susceptible to overheating because of their broader energy band gap, and they also tend to produce less noise (disturbance in an electrical signal) in electronic circuits in comparison with silicon devices, more stable over long-time and reasonably priced [21]. Furthermore, the dependency of thicknesses of absorber layer and that of temperature of these performance parameters has also been investigated in this study. Several studies on dilute nitrides based solar cells have already been reported previously where reported efficiency is far below the anticipated value [22-24]. Therefore, the purpose of this research is to optimize absorption layer material properties and structures of thin-film solar cell towards high efficiency thin-film solar cells.

There are five sections in the paper. The research work of this paper is briefly introduced in the section I. Methods and techniques including suggested thin-film solar cell construction and modelling approach will be covered in section II. Analysis and optimization of V_{oc} , J_{sc} , FF and η for different band gap energies, absorber layer thickness, operating temperature, and work function of back contact of the thin-film solar cell are shown in section III. The findings will be briefly concluded in section IV.

2. Methods and Methodology

The suggested thin-film solar cell structure, n-GaAs/p-GaAsN/p⁺-GaAs has been depicted schematically in Figure 1. Three-layered structure is taken into consideration in this study where the uppermost n-type GaAs layer as buffer layer, middle p-type GaAs_{1-x}N_x with zinc blende crystal structure as absorber layer and the bottom most highly doped p-type GaAs as hole transport layer (HTL). A pn-junction is formed by the n-type GaAs layer and the p-type GaAs_{1-x}N_x absorber layer, thereafter a depletion layer is developed at that junction. The solar cells are illuminated under 1000 mW/cm² with global air mass AM1.5 G spectrum of the solar radiation at operating temperature 300 K. We have taken into account optimal circumstances for the series (R_s) and shunt (R_{sh}) resistances of the suggested solar cell structure.

One of the most widely used and trustworthy computer simulation tools titled, “Solar Cell Capacitance Simulator’s one-dimensional simulation software (SCAPS-1D)” has been used to simulate the suggested structure and examine the performance characteristics. Burgelman et al of the Department of Electronics and Information Systems, University of Gent, Belgium invented the program [25], especially for thin-film solar cell. Solar cell researchers have the chance to efficiently examine the device structure by using this program [26, 27]. Electrical characterizations and spectral responses of solar cells can be performed with this very helpful tool. SCAPS-1D program determines the solar cell’s performance parameters by using numerical solutions of the Poisson’s equation and the continuity equation for semiconductors. Many researchers have already found good agreement between the experimental result and SCAPS-1D theoretical simulation result for thin-film solar cells structure.

As mentioned earlier, dilute nitrides semiconductor $\text{GaAs}_{1-x}\text{N}_x$ has been used as absorber layer in our study because of its unique optical properties such as nitrogen concentration dependence large band gap bowing. Figure 2(a) and 2(b) showed nitrogen (N) and arsenium (As) concentration dependence band gap energy of $\text{GaAs}_{1-x}\text{N}_x$ that had been extracted from reference [17].

As can be seen from these Figure 2(a) and 2(b), the band gap energy of $\text{GaAs}_{1-x}\text{N}_x$ dramatically changes with increasing the percentage of N- or conversely with decreasing As composition in this alloy. When the values of x are 0 and 1, it acts as GaAs and GaN, respectively. Thus, desirable band gap energy can be obtained by tuning N or As concentration in this alloy. For example, the lowest band gap energy of $\text{GaAs}_{1-x}\text{N}_x$ can be obtained as 0.4 eV by choosing 45% ($x = 0.45$) N atoms with respect to As atoms in this alloy.

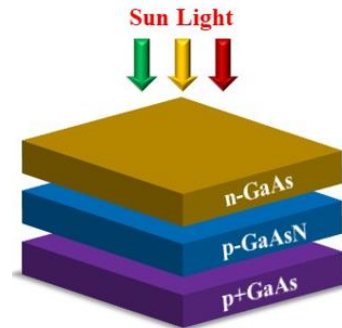


Figure 1. Schematic diagram of suggested thin-film solar cell, n-GaAs /p-GaAsN/p+-GaAs.

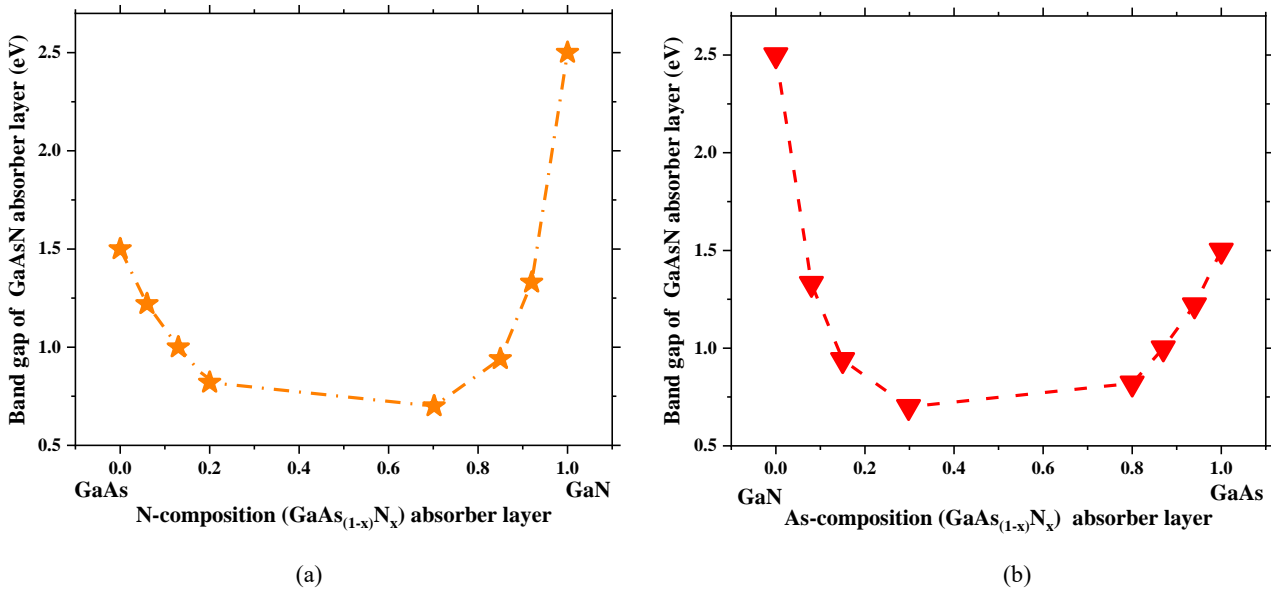


Figure 2. (a) Nitrogen and, (b) Arsenium concentration dependence band gap energy of $\text{GaAs}_{1-x}\text{N}_x$ extracted from reference [17].

Table 1 lists thin-film solar cell parameters that were used to calculate our numerical simulations based on the previously examined research studies.

Table 1. Numerical values of various parameters considered in this investigation.

Symbols	Parameters	GaAs	GaAs _{1-x} N _x
σ	Conductivity	p ⁺ /n	p
W	Thickness (nm)	20/1000	500-3000
E_g	Band gap energy (eV)	1.42 [28]	0.7-1.5 [17]
χ	Electron affinity (eV)	4.07 [28]	4.071 [28]
ϵ_r	Relative dielectric permittivity	12.5 [28]	12.38 [28]
N_C	Effective conduction band density (cm ⁻³)	4.33×10 ¹⁷ [28]	4.66×10 ¹⁷ [28]
N_V	Effective valance band density (cm ⁻³)	1.28×10 ¹⁹	1.39×10 ¹⁹
μ_n	Mobility of electron (cm ² V ⁻¹ s ⁻¹)	8500 [28]	6538.46 [28]
μ_p	Mobility of hole (cm ² V ⁻¹ s ⁻¹)	400 [28]	397.72 [28]
N_D	Concentration of donor (cm ⁻³)	1.0×10 ¹⁶ / 1.0×10 ¹⁸ [28]	0
N_A	Concentration of acceptor (cm ⁻³)	5.0×10 ¹⁹ / 5.0×10 ¹⁹ [28]	1×10 ¹⁶

3. Results and Discussions

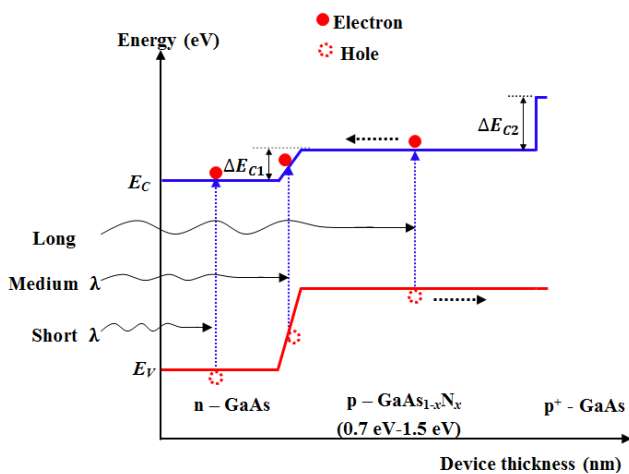


Figure 3. Schematic energy band diagram of the proposed thin-film solar cell structure with possible optical transitions.

Using SCAPS-1D software, the suggested thin-film solar cell structure has been simulated. Figure 3 shows the schematic energy band diagram of this proposed structure with possible optical transitions. Medium and lower energy or longer wavelength photons are primarily absorbed within the depletion region and within the p-GaAs_{1-x}N_x absorber layer, respectively, whereas incident photons with energy greater than 1.42 eV are possibly absorbed by the n-GaAs layer due its 1.42 eV band gap energy. The band gap energy and thickness of the absorber layer play a vital role in this situation.

By the way, incident solar energy creates electron-hole pairs in these areas of solar cell. The n- side region becomes negative when electron moves in the direction of n-side. In a same manner, the hole moves in the direction of the p⁺ side, making it positive. The greater likelihood of carrier collection across the load terminals is confirmed by the fact that the diffusion length of electron should be longer than that of hole because electrons have a higher mobility and lifetime than holes. Thus, the effects of band gap energy and thickness of absorber layer on the performance parameters have been considered in this study. The p⁺ GaAs layer allows holes to go towards the back electrode while blocking electron flow by creating a potential barrier (ΔE_{C2}). This research has been done to demonstrate enhancement of conversion efficiency of the dilute nitrides based GaAs_{1-x}N_x thin-film solar cell. Band gap energy and thickness of absorber layer p-GaAs_{1-x}N_x as well as operating temperature, work function of back contact were optimized in this study to fabricate a high efficiency solar cell with reduced fabrication time and cost, thus enhance production throughput.

3.1. Band Gap Energy Tuning of GaAs_{1-x}N_x by Adjusting N-concentrations for Getting Optimized Values of V_{oc} , J_{sc} , FF and η

We have firstly studied the effects of bang gap energy of dilute nitrides semiconductor based absorber layer on the essential performance metrics of photovoltaic cells. To achieve optimized values of V_{oc} , J_{sc} , FF and η from the proposed thin-film solar cell for different nitrogen concentration of absorber layer GaAs_{1-x}N_x, the four performance parameters have been investigated as a function of band gap energy of this layer on the same horizontal axis as visualized

in Figure 4. Interesting behaviors have been observed in all fundamental parameters of the thin-film solar cell for changing band gap energy of dilute nitrides semiconductor, $\text{GaAs}_{1-x}\text{N}_x$.

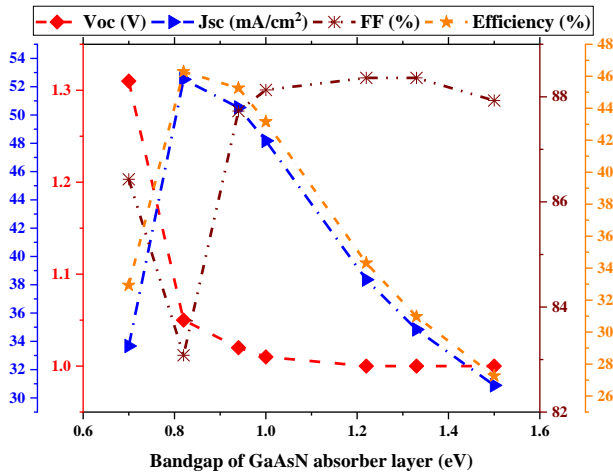


Figure 4. V_{oc} , J_{sc} , FF and η of thin-film solar cell as a function band gap energy of absorber layer, $\text{GaAs}_{1-x}\text{N}_x$.

It was observed in the figure that the short-circuit current density and efficiency had showed similar tendency with increasing band gap energy of $\text{GaAs}_{1-x}\text{N}_x$ layer while FF had showed variation in different ways in the whole range of band gap energy considered in this study. As can be seen from Figure 4, both J_{sc} and η rapidly increased in a similar manner on their respective scales with increasing band gap energy up to 0.82 eV which corresponds to the nitrogen concentrations of approximately 17% ($x = 0.17$) and 83% ($x = 0.83$) in $\text{GaAs}_{1-x}\text{N}_x$. The maximum values of J_{sc} and η have been obtained as about 53 mA/cm^2 and 46%, respectively at that band gap energy. Due to the opposite changing tendency of FF with respect to J_{sc} and η , the minimum value of FF have been achieved which is about 32% at that particular band gap energy. Above that threshold band gap energy, both J_{sc} and η started decreasing while FF increased in an exponential manner with increasing band gap energy. Finally, J_{sc} and η became the lowest at band gap energy 1.7 eV which can be obtained by adjusting nitrogen concentration either about 23% ($x = 0.23$) or 94% ($x = 0.94$) into $\text{GaAs}_{1-x}\text{N}_x$ as can be seen from Figure 2a. Dissimilar to J_{sc} , η and FF , open circuit voltage V_{oc} is found decreasing abruptly with increasing band gap energy of $\text{GaAs}_{1-x}\text{N}_x$ layer from 0.7 eV to 0.82 eV in this study, and then being saturated with respect to band gap energy of absorber layer.

As the energy gap of $\text{GaAs}_{1-x}\text{N}_x$ layer increases from 0.7 eV to 0.82 eV, the valence band E_v shifts downward while the conduction band E_c shifts upwards and consequently the value of conduction band offset (ΔE_{C1}) increases. The higher conduction band offset ΔE_{C1} shown in Figure 3 affects the depletion

region at the junction which in turn makes easy the charge diffusion process and helps to reduce carrier recombination rate in the active region and therefore enhances the value of J_{sc} and η . If the band gap energy continuously increases to higher value, the photon with lower energy could not be absorbed in the absorption layer. In addition, the density of carrier concentrations close to the interface junction and surface boundary becomes adequate, therefore the probability of carrier recombination through surface and interface increases drastically. Consequently, demotion in the short circuit current density [29] and efficiency of the thin-film solar cell occurs at the higher band gap energy of absorber layer. Since the excess carriers may perhaps vanish by recombination process at surface and interface at higher band gap energy of absorber layer, the open circuit voltage might be saturated due to the fact. Thus we concluded that lower band gap energy i.e. 0.82 eV of dilute nitrides based absorber layer $\text{GaAs}_{1-x}\text{N}_x$ is preferable for obtaining higher efficiency as 46% with optimized values of V_{oc} , J_{sc} and FF of solar cells.

It can be noted here that same band gap energy can possibly be obtained at different nitrogen concentrations in $\text{GaAs}_{1-x}\text{N}_x$ because of having nitrogen concentration dependence unconventional large band gap bowing characteristics of dilute nitrides semiconductors. For examples, although it is possible to obtain 0.82 eV band gap energy at approximately 17% and 83% of nitrogen concentrations in $\text{GaAs}_{1-x}\text{N}_x$, it is suggested to choose lower nitrogen concentration as 17% in dilute nitrides for getting that band gap energy because of several prominent advantageous. The top and bottom of the absorber layer are n-GaAs layer and p⁺-GaAs hole transport layer, respectively in the proposed structure as shown in Figure 1. As the lattice parameter of GaAs is 5.65 Å, the lattice mismatch of $\text{GaAs}_{1-x}\text{N}_x$ to GaAs increases with increasing nitrogen concentration. The probability of occurring misfit dislocation acting as recombination centers increases at the GaAs/ $\text{GaAs}_{1-x}\text{N}_x$ interface with increasing lattice mismatch between them. Nevertheless, samples of $\text{GaAs}_{1-x}\text{N}_x$ with higher nitrogen concentration are abounded with many as-grown defects [30-32] which suggested that reliable performance could not be expected from those samples. Previous study on GaAsN alloy also revealed that the photoluminescence (PL) intensity improvement occurs in this alloy during laser irradiation [20] which is an evidence of the reliability and longer life-time during operation. Since nitrogen concentration determines the band gap energy and other important properties of the dilute nitrides $\text{GaAs}_{1-x}\text{N}_x$, there is an exceptional feasibility such as lower density of as-grown defects, longer lifetime or greater reliability in dilute nitrides based thin-film solar cell structure for getting optimized values of V_{oc} , I_{sc} , FF and η as well.

3.2. Optimization of V_{oc} , J_{sc} , FF and η for the Different Thickness of $\text{GaAs}_{1-x}\text{N}_x$ Absorber Layer of Thin-Film Solar Cell

One of the most crucial factors for improving the solar cell

performance is the absorber layer's thickness. The thickness of the absorber layer is one of the most important parameters in increasing the performance of solar cells [33]. In this section, the absorber layer thickness of the proposed structure has been optimized for achieving improved V_{oc} , J_{sc} , FF and η . In order to illustrate this, the performance characteristics of the thin film solar cell have been plotted as a function of thickness of absorber layer $GaAs_{1-x}N_x$ as shown in Figure 5.

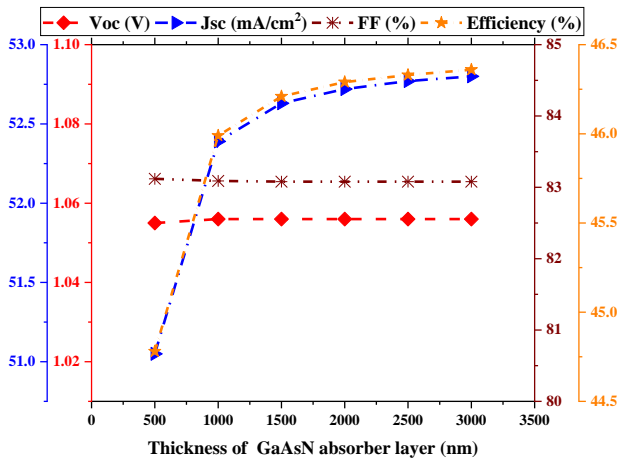


Figure 5. Dependency of V_{oc} , J_{sc} , FF and η parameters on the thickness of $GaAs_{1-x}N_x$ absorber layer of thin-film solar cell.

As seen from the figure, V_{oc} and FF showed similar and nearly saturated behavior with increasing absorber layer thickness. On the other hand, both J_{sc} and η increases exponentially with increasing thickness of $GaAs_{1-x}N_x$ absorbing layer. As can be seen from the Figure 5 that at 500 nm thickness of absorber layer, the V_{oc} and FF are about 1.057 V and 45.75% respectively. If the thickness increased, the values of these two parameters remained relatively unchanged. Even at the 3000 nm thickness, the values V_{oc} and FF still were found the same like at 500 nm. The values of both J_{sc} and η rose rapidly on their respective scales for increasing of thickness in the lower range. As seen from Figure 5, the J_{sc} increased from 51.1 to 52.37 V while η raised from 44.75% to 45.95% for the thickness change from 500 nm to 1000 nm. The results can be explained by the fact that photon absorption of incident light in this location increases with increasing absorber layer's thickness which results in extra electron-hole pair generation, and, in turn, boosts short circuit current density and efficiency. A few hundred nanometer film of GaAsN material can absorb enough sunlight because of its high-absorption coefficient [19]. As a result, the increase in J_{sc} and η is shown to be more substantial for the increase in absorber layer's thickness in the lower range from 500 nm to 1000 nm. In tandem with the improvement of light absorption, the probability of carrier recombination also rises with increasing thickness of absorber layer because of longer carrier diffusion length in a

thicker absorber layer. As a result, the photocurrent density and efficiency gradually increase with thickness above 1000 nm and eventually reach saturation at a thickness of roughly 2500 nm for the absorber layer. However, the open circuit voltage stayed relatively constant in this situation. As the thickness of absorber layer increased, the carrier diffusion length, the probability of photo-generated carrier's recombination rate and built-in barrier potential also increased, affecting the life-time of photo-generated carrier and, in turn V_{oc} . Therefore, the domination of the carrier recombination process and decreased carrier extraction with increasing thickness may be the cause of the saturation in V_{oc} . The behavior of the FF is likely similar to that of V_{oc} [34]. The efficiency behavior could be illustrated by the behavior and values of V_{oc} , J_{sc} and FF [35]. Since V_{oc} and FF have slight variation with increasing absorber layer thickness, thereby the efficiency follows the similar exponential shape as J_{sc} as shown in Figure 5. Therefore, we have determined that the ideal thickness of $GaAs_{1-x}N_x$ absorber layer is around 2000 nm due to better performance parameters values.

3.3. Evaluation of Temperature Effects on V_{oc} , J_{sc} , FF and η of Dilute Nitrides $GaAs_{1-x}N_x$ Based Thin-Film Solar Cell

The performance of the solar cells is significantly impacted by operating temperature [36]. In this study, all simulations have been carried-out by considering temperature at 300 K which is averaged room temperature of our country. The temperature was raised from 290 K to 330 K in this section to account for the impact of the operating temperature on V_{oc} , J_{sc} , FF and η performances of dilute nitrides $GaAs_{1-x}N_x$ based thin-film solar cells as demonstrated in Figure 6. It should be mentioned that the temperature range utilized in this section is consistency with the range that exists from winter to the summer in Bangladesh.

It can be seen from the Figure 6 that the temperature change in our study had a significant impact on all parameters except current density function. The value of J_{sc} is found nearly temperature independent which is about 52.52 mA/cm². It has been noticed that V_{oc} , FF and η showed up rising tendency with increasing temperature up to 300 K while after that temperature, they showed opposite trend with temperature rise. At 300 K, the values of V_{oc} and η are about 1.66 V and 46.28%, respectively which are the maximum values of the respective parameters obtained from temperature dependence performance evaluation in this study. These findings can be explained by the fact that the increase in temperature up to 300 K were advantageous because they may have accelerated electron-hole pair generation through the transfer of heat energy and increase the rate of carrier diffusion. However, if the temperature rises steadily to higher range, it starts to adversely solar cell performance by altering several parameters of materials at once.

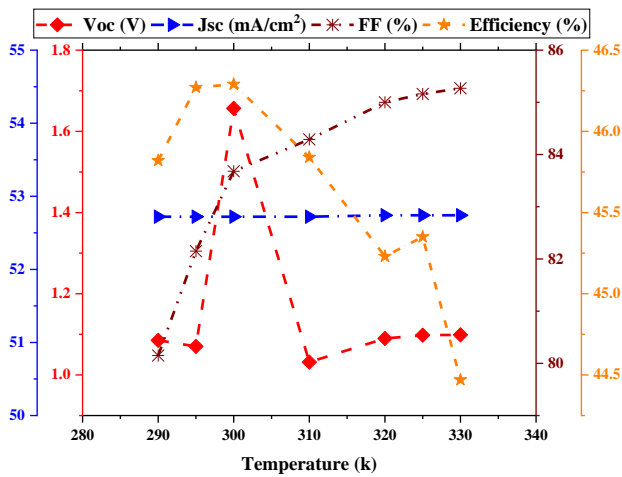


Figure 6. Temperature effects on V_{oc} , J_{sc} , FF and η of dilute nitrides $GaAs_{1-x}N_x$ based thin-film solar cell.

Elevated temperature causes the band gap energy of the dilute nitrides to shift to lower energy [37], enhance the velocity-instability of charged particles [38], reverse the material's resistivity and saturation current. Degradation of V_{oc} finally takes place as a result of raising charge carrier recombination rate prior to reaching the depletion region. Device ohmic losses, including series and shunt resistances, metal contact and recombination losses can limit the value of J_{sc} . It would appear from the consistent current density with the temperature that the combined influence of the aforementioned parameters could reduce the fluctuation in J_{sc} in our simulation. Furthermore, FF increases with increasing temperature in the whole range although the increment is more significant below 300 K. The behavior of the FF is potentially reliant on the joint actions of V_{oc} and J_{sc} [39, 40]. Constant J_{sc} and rapid increase in V_{oc} together resulted in rapid increase in FF of the device up to 300 K while that but decrement in V_{oc} caused resultant gradual rise in FF with increasing temperature above 300 K. The overall behavior of V_{oc} , J_{sc} and FF is reflected in the value of η . Constant J_{sc} and increment in both V_{oc} and FF indicating a path for raising device's η up to 300 K. Since J_{sc} remained nearly constant, V_{oc} rapidly decreased while FF slowly increased with increasing temperature after 300 K, thereby the efficiency followed middle paths between V_{oc} and FF i.e. slower decrement than V_{oc} as shown in Figure 6. Therefore we proposed to operate thin-film solar cell at temperature 300 K for obtaining better performances.

3.4. Optimization of V_{oc} , J_{sc} , FF and η by the Work Function of Back Metal Contact at 0.82 eV Band Gap of Absorber Layer

The electric field produced at the depletion region separates carriers, which are finally collected by the electrodes or metal contacts eventually creating flow of current towards the load. Defectiveness in the metal-semiconductor interface as well as

the work functions of the front and back electrodes have an critical role to promote/demote photo-generated carriers, stability and consequently in raising or lowering the performance efficiency of the thin-film solar cells [27, 41]. Materials used as back contact include magnesium (Mg), copper (Cu), carbon (C), molybdenum (Mo), beryllium (Be), nickel (Ni), zinc (Zn), aluminum (Al) and gold (Au) with different work functions [42]. The work function of back metal contact or electrode dependence characteristics curves of V_{oc} , J_{sc} , FF and η at 0.82 eV band gap energy of absorber layer $GaAs_{1-x}N_x$ have been visualized in Figure 7.

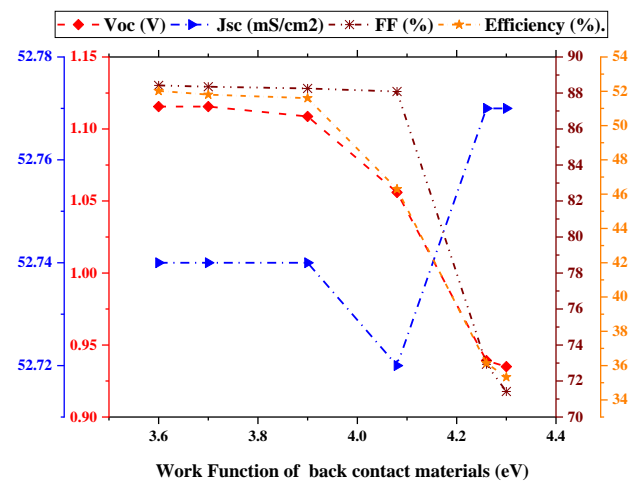


Figure 7. Work function of back metal contact dependence V_{oc} , J_{sc} , FF and η at 0.82 eV band gap energy of absorber layer $GaAs_{1-x}N_x$.

It was found that the behaviors of V_{oc} , FF and η are nearly comparable in the whole range of metal contact work function from 3.6 eV to 4.2 eV at 0.82 eV band gap energy of $GaAs_{1-x}N_x$ considered in this study. Although J_{sc} showed similar changing tendency like V_{oc} , FF and η with increasing work function of electrode from 3.6 eV to 4.08 eV, however, it suddenly started opposite changing behavior in contrast to V_{oc} , FF and η after 4.08 eV of electrode work function. All of these performance metrics stayed roughly constant on their respective scales for a specific range of electrode work function from 3.6 eV to 3.9 eV, as shown in Figure 7. After that range, the slowly degradation behavior has been observed in all parameters till 4.08 eV. Furthermore, rapid degradation in V_{oc} , FF and η while dramatic uprising in J_{sc} occurred as the work function of metal contact increased from 4.08 eV to 4.2 eV. Maximum values of V_{oc} , FF and η were obtained as 1.12 V, 88.5% and 52% respectively at the lower work function such as 3.6 eV while oppositely that of J_{sc} (52.77 mA/cm²) was gotten at about higher work function of electrode (4.3 eV).

Energy band diagram of the device can be used to demon-

strate clearly the effects of work function on the device performance parameters. The metal contact at the semiconductor device presents equivalently ohmic resistance and acts as potential barrier to impede carrier diffusion. As can be seen from Figure 3, when the work-function of the electrode increases, potential barrier also decreases. The electrode’s lower work function in this device structure may ensure better device’s performance because the reduced potential barrier makes it easier for more carriers to pass across the junction. Due to special advantages, we have chosen aluminium (Al) metal whose work function is 4.08 eV to be used as a back metal contact or anode in our proposed solar panel [43].

3.5. Optimization of V_{oc} , J_{sc} , FF and η by the Work Function of Metal Contact at 0.7 eV Band Gap of Absorber Layer

Like to section 3.4, similar simulation has also been carried out in this section but band gap energy of absorber layer GaAs_{1-x}N_x was kept 0.7 eV as illustrated in Figure 8 in order to explore the dependence of V_{oc} , J_{sc} , FF and η on metal contact work function at different band gap energy of absorber layer. It is interesting to investigate from Figure 8 that not only V_{oc} , FF and η but also J_{sc} showed nearly similar varying tendency in the whole range of metal contact work function at 0.7 eV band gap energy of GaAs_{1-x}N_x considered in this study. By making comparison between Figures 7 and 8, it was boldly noticed that the correlation between absorber layer band gap energy and back electrode work function has significant effects on the short circuit density of solar cells. For example, with increasing work function of electrode from 3.6 eV to 4.08 eV, complementary behaviors i.e. upgradation and degradation in short circuit density have been investigated at band gap energy of absorber layer 0.82 eV and 0.7 eV, respectively.

Similar to Figure 7, little bit or very slowly degradation behavior has been observed in all other parameters with increasing energy of work function in the range from 3.6 eV to 3.9 eV as shown in Figure 8.

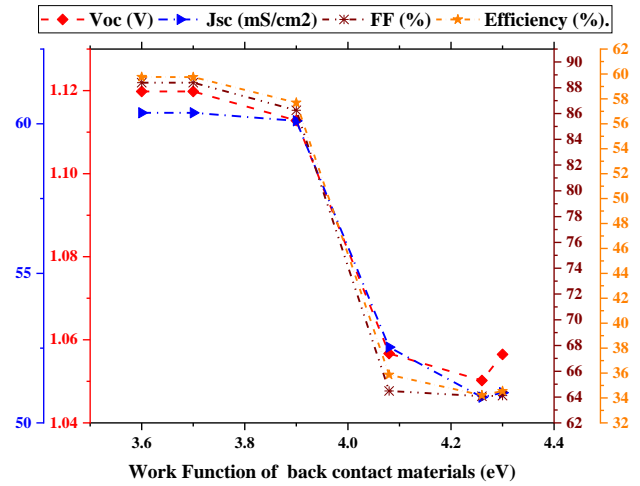


Figure 8. Evaluation of V_{oc} , J_{sc} , FF and η at 0.7 eV band gap energy of absorber layer GaAs_{1-x}N_x as a function of work function of back metal contact.

The degradation amount became more significant after work function 3.9 eV. Furthermore, the degradation in V_{oc} , J_{sc} , FF and η became slower after 4.08 eV with increasing energy of work function. The best and optimized values of V_{oc} , J_{sc} , FF and η have been obtained at 3.7 eV of metal contact work function while the band gap energy of absorber layer GaAs_{1-x}N_x have been tuned to 0.7 eV by adjusting nitrogen concentration in this layer.

3.6. Comparison Among Photovoltaic Parameters of the Suggested Model with the Relevant Models Reported Previously

Finally, we have attempted to compare the performance parameters of our suggested model with those of the relevant models previously reported by other researchers, as indicated in Table 2.

Table 2. Comparison of the solar cell’s photovoltaic characteristics related to GaAs-based absorber layer.

Thin-film solar cell structure	V_{oc} (V)	J_{sc} ($\frac{mA}{cm^2}$)	FF (%)	η (%)	References
n-GaAs/p-GaAsN/p ⁺ -GaAs	~1.10	~53	~88	~46	proposed
p ⁺ -GaAs/p ⁺ -AlGaAs/p-GaAsN/ n-AlGaAs/n ⁺ -GaAs	1.105	44.22	89.84	43.90	[22]
p-GaAs/p-GaAs/n-GaAs	0.930	30.31	--	24.94	[28]
p-GaAsN/n-GaAsN	0.79	68.00	68.0	38.20	[44]
n ⁺ -GaAs/n ⁺ -GaAsN/p-GaAsN	0.80	25.00	76.0	15.00	[23]
n-GaAs/p-GaAsN/n-GaAs	1.053	44.80	84.89	43.90	[22]

From our suggested thin-film solar cell, it is possible to achieve comparatively higher open circuit voltage, short-circuited current density, fill-factor and efficiency.

4. Conclusions

Solar Cell Capacitance Simulator in one dimensional (SCAPS-1D) software was used in this study to simulate the thin-film solar cell construction with unique dilute nitride GaAs_{1-x}N_x as an absorber layer's material. The four basic performance metrics including V_{oc} , J_{sc} , FF and η have been examined and adjusted by using band-gap bowing characteristics of GaAs_{1-x}N_x and various absorber layer's thickness as well as several working temperatures, work functions of back contact. The performances studied on various absorber layer's band gap energy exposed that the maximum efficiency more than 46% was achieved from the proposed structure by tuning band gap energy to 0.82 eV which is possible to obtain via adjusting nitrogen concentration into dilute nitrides GaAs_{1-x}N_x at either approximately 17% or 83%. In this study, it is suggested to choose lower nitrogen concentration for getting that band gap energy because of having some advantageous, such as lower density of as-grown defects and reliable lifetime. The study of performance factors for different absorber layer's thicknesses has made it clear that a thickness of about 2000nm is ideal for improving the suggested solar cell's efficiency. Furthermore, research on efficiency and other performance metrics at temperature between 290 K to 330 K has revealed that 330 K is the ideal operating for solar cell to ensure steady functioning. Lastly, by assessing the influence of V_{oc} , J_{sc} , FF and η on metal contact work function at various absorber layer's band gap energy, it was discovered that J_{sc} changed significantly as the absorber layer's band gap energy changed. The results of this study would be very beneficial for the development of the renewable energy technology in the nanometer range. That's the way, it's outcome would play a significant role for reducing global energy crisis and green-house gas emission at once in a sustainable manner. There is still research opportunity in future for further performance improvement by adding additional layers with precious materials to this suggested structure.

5. Highlights of the Article

- 1) Very popular dilute nitrides, GaAs_{1-x}N_x based structure of thin-film solar cell has been modelled and optimized by using SCAPS-1D.

- 2) Efficiency around 46% can be achieved by tuning bandgap energy to 0.82eV of absorber layer material GaAs_{1-x}N_x.
- 3) Bandgap bowing of GaAs_{1-x}N_x gives us the feasibility to achieve 0.82eV bandgap energy by adjusting nitrogen concentrations approximately 17% ($x = 0.17$) and 83% ($x = 0.83$) in GaAs_{1-x}N_x. Since the density of as-grown defects is lower in GaAs_{1-x}N_x with $x = 0.17$ than 0.83, it is suggested to use lower nitrogen concentration in GaAs_{1-x}N_x to obtain the efficiency.
- 4) The study also encompasses an exploration of the open-circuited voltage (V_{oc}), short-circuited current density (J_{sc}) and fill-factor (FF) performance parameters.
- 5) By precisely evaluation of the performance metrics for several absorber layer thickness indicated that a thickness of about 2000nm is appropriate for achieving higher efficiency.
- 6) Furthermore, increased efficiency and improved other performance metrics were obtained at temperature 300K.

Graphical Abstract

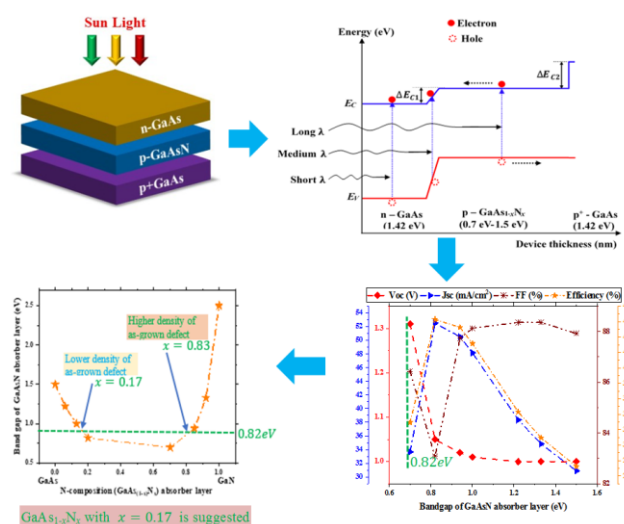


Figure 9. Graphical Abstract.

Abbreviations

GHGs	Green-House Gases
V_{oc}	Open-circuited Voltage
J_{sc}	Short-circuited Current Density

*Corresponding author: mdzamilsultan@hstu.ac.bd (Zamil Sultan)

Received: 8 October 2024; Accepted: 12 November 2024; Published: 29 November 2024



FF	Fill-factor
η	Efficiency
SCAPS-1D	Solar Cell Capacitance Simulator's One-dimensional Simulation Software
eV	Electron Volt
K	Kelvin

Acknowledgments

We are grateful to the Department of Electrical and Electronic Engineering, Hajee Mohammad Danesh Science and Technology University, Dinajpur-5200, Bangladesh for providing necessary technical supports.

Author Contributions

Zamil Sultan: Conceptualization, Investigation, Methodology, Supervision, Validation, Visualization, Writing – review & editing

Nuralam Howlader: Conceptualization, Data curation, Formal Analysis, Investigation, Methodology, Software, Visualization, Writing – original draft

Forhad Hossen: Investigation, Software, Validation, Visualization

Asaduzzaman Joy: Conceptualization, Data curation, Formal Analysis, Investigation, Methodology, Resources, Software, Visualization, Writing – original draft

Asadul Haque: Conceptualization, Formal Analysis, Investigation, Methodology, Software, Visualization, Writing – original draft

Funding

The research was carried-out by self-funded.

Disclosure

No conflicts of interest are disclosed by the writers.

Data Availability Statement

The corresponding author can provide the study's data upon reasonable request.

Conflicts of Interest

The authors declare no conflicts of interest.

References

- [1] Owusu, P. A. & Asumadu-sarkodie, S. sustainability issues and climate change mitigation A review of renewable energy sources, sustainability issues and climate change mitigation. *Cogent Eng.* 15, (2016).
- [2] Ebhota, W S, and Jen, T.-C. Fossil Fuels Environmental Challenges and the Role of Solar Photovoltaic Technology Advances in Fast Tracking Hybrid Renewable Energy System. *Int. J. Precis. Eng. Manuf. Technol.* 7, 97–117 (2019).
- [3] Shiyani, T., Mahapatra, S. K. & Banerjee, I. Plasmonic Solar Cells. *Fundam. Sol. Cell Des.* 16, 55–81 (2023).
- [4] Bilgen, S. Structure and environmental impact of global energy consumption. *Renew. Sustain. Energy Rev.* 38, 890–902 (2014).
- [5] Islam, M. M. & Hasanuzzaman, M. Introduction to energy and sustainable development. *Energy Sustain. Dev. Demand, Supply, Convers. Manag.* 1–18 (2020)
<https://doi.org/10.1016/B978-0-12-814645-3.00001-8>
- [6] Lhoussayne Et-taya, Touria Ouslimane, A. B. Numerical analysis of earth-abundant $\text{Cu}_2\text{ZnSn}(\text{SxSe}_{1-x})_4$ solar cells based on Spectroscopic Ellipsometry results by using SCAPS-1D. *Sol. Energy* 201, 827–835 (2020).
- [7] NREL. Documenting a Decade of Cost Declines for PV Systems Documenting a Decade of Cost Declines for PV Systems, The National Renewable Energy Laboratory (NREL). 23–25 (2021).
- [8] Fangchao Li, Sijie Zhou, Jianyu Yuan, Chaochao Qin, Yingguo Yang, Junwei Shi, Xufeng Ling, Youyong Li, and W. M. Perovskite Quantum Dot Solar Cells with 15.6% Efficiency and Improved Stability Enabled by an α - $\text{CsPbI}_3/\text{FAPbI}_3$ Bilayer Structure. *ACS Energy Lett.* 4, 2571–2578 (2019).
- [9] Yasodharan R, Senthilkumar A. P, Mohankumar P, Ajayan J, S. R. Investigation and influence of layer composition of tandem perovskite solar cells for applications in future renewable and sustainable energy. *Optik (Stuttg.)* 212, 164723 (2020).
- [10] Mazzucato, S. *et al.* Dilute nitride and GaAs n-i-p-i solar cells. *Nanoscale Res. Lett.* 7, 1–5 (2012).
- [11] Deshpande, R. A. Advances in Solar Cell Technology: An Overview. *J. Sci. Res.* 65, 72–75 (2021).
- [12] Moon, S., Kim, K., Kim, Y., Heo, J. & Lee, J. Highly efficient single-junction GaAs thin-film solar cell on flexible substrate. *Sci. Reports, Nat. Publ. Gr.* 6, 1–6 (2016).
- [13] Elshorbagy, M. H., Abdel-Hady, K., Kamal, H. & Alda, J. Broadband anti-reflection coating using dielectric Si_3N_4 nanostructures. Application to amorphous-Si-H solar cells. *Opt. Commun.* 390, 130–136 (2017).
- [14] Bi, W. G. & Tu, C. W. Bowing parameter of the band-gap energy of $\text{Ga}_x\text{As}_{1-x}$. *Appl. Phys. Lett.* 70, 1608–1610 (1997).
- [15] Miyoshi, S., Yaguchi, H., Onabe, K., Ito, R. & Shiraki, Y. Metalorganic vapor phase epitaxy of $\text{GaP}_{1-x}\text{N}_x$ alloys on GaP. *Appl. Phys. Lett.* 63, 3506 (1993).

- [16] Luque, A. & Martí, A. Increasing the Efficiency of Ideal Solar Cells by Photon Induced Transitions at Intermediate Levels. *Phys. Rev. Lett.* 78, 5014 (1997).
- [17] Bellaiche, L., Wei, S. H. & Zunger, A. Band gaps of GaPN and GaAsN alloys. *Appl. Phys. Lett.* 70, 3558–3560 (1997).
- [18] Weyers, M. *et al.* N incorporation in InP and band gap bowing of InN_xP_{1-x}. *Appl. Phys. Lett.* 80, 1934 (1992).
- [19] Weyers, M., Sato, M. & Ando, H. Red shift of photoluminescence and absorption in dilute GaAsN alloy layers. *Jpn. J. Appl. Phys.* 31, L853 (1992).
- [20] Yaguchi, H. *et al.* Improvement in the luminescence efficiency of GaAsN alloys by photoexcitation. *Phys. Status Solidi C* 0, 2782 (2003).
- [21] Lin, Q. *et al.* Flexible photovoltaic technologies. *J. Mater. Chem. C* 2, 1233–1247 (2014).
- [22] Haque, D., Ali, H., Halim, A. & Islam, A Z M Touhidul, Hossain, Md Mahabub, and H. M. I. Design and Simulation of GaAsN Based Solar Cell with AlGaAs blocking layer for Harvesting Visible to Near-infrared Light. *Phys. Scr.* 97, 085006 (2022).
- [23] Wang, L., Elleuch, O., Kojima, N., Ohshita, Y. & Yamaguchi, M. Simulation analysis of the potential causes for the low Jsc in GaAsN solar cells. in *International Conference on Solid State Devices and Materials* 390–391 (2014). <https://doi.org/10.7567/SSDM.2014.PS-15-1>
- [24] Krispin, P., Gambin, V., Harris, J. S., Ploog, P. K. H. Nitrogen-related electron traps in Ga (As, N) layers ($\leq 3\%$ N). *J. Appl. Phys.* 93, 6095–6099 (2003).
- [25] Verschraegen, J., Burgelman, M. Numerical modeling of intra-band tunneling for heterojunction solar cells in scaps. *Thin Solid Films* 515, 6276 (2007).
- [26] Hima, A, Lakhdar, N. Enhancement of efficiency and stability of CH₃NH₃GeI₃ solar cells with CuSbS₂. *Opt. Mater. (Amst)*. 99, 109607 (2020).
- [27] Pindolia, G., Shinde, S. M. & Jha, P. K. Optimization of an inorganic lead free RbGeI₃ based perovskite solar cell by SCAPS-1D simulation Optimization of an inorganic lead free RbGeI₃ based perovskite solar cell by SCAPS-1D simulation. *Sol. Energy* 236, 802–821 (2022).
- [28] Boumesjed, A., Mazari, H., Ameer, K. Predicted Theoretical Efficiency For New Intermediate Band Solar Cells (IBSC) Based On GaAs_{1-x}N_x. *J. New Technol. Mater.* 8, 102–109 (2018).
- [29] Moustafa, M., Al Zoubi, T. & Yasin, S. Exploration of CZTS-based solar using the ZrS₂ as a novel buffer layer by SCAPS simulation. *Opt. Mater. (Amst)*. 124, 112001 (2022).
- [30] Zhang, S. B. & Wei, S. H. Nitrogen solubility and N-induced defect complexes in epitaxial GaAs:N. *Phys. B* 308–310, 839–842 (2001).
- [31] Zhang, S. B. & Wei, S. H. Nitrogen solubility and induced defect complexes in epitaxial GaAs:N. *Phys. Rev. Lett.* 86, 1789–1792 (2001).
- [32] Bouzazi, B., Kojima, N., Ohshita, Y. & Yamaguchi, M. Effect of electron and proton irradiation on recombination centers in GaAsN grown by chemical beam epitaxy. *Curr. Appl. Phys.* 13, 1269–1274 (2013).
- [33] Ouslimane, T., Et-taya, L., Elmaimouni, L. & Benami, A. Impact of absorber layer thickness, defect density, and operating temperature on the performance of MAPbI₃ solar cells based on ZnO electron transporting material. *Heliyon* 7, e06379 (2021).
- [34] Mbopda Tcheum, G. L.; Teyou Ngoupo, A.; Ouédraogo, S.; Guirdjebaye, N.; Ndjaka, J. M. B. Numerical analysis of ultrathin Cu (In,Ga)Se₂ solar cells with Zn (O,S) buffer layer. *Pramana* 94, 111 (2020).
- [35] Baloch, A. A. B., Aly, S. P., Hossain, M. I. & El-mellouhi, F. Full space device optimization for solar cells. *Sci. Rep.* 7, 11984 (2017).
- [36] Daoudia, A. K., Hassouani, Y. El & Benami, A. Investigation of the effect of thickness, band gap and temperature on the efficiency of CIGS solar cells through SCAPS-1D. *Int. J. Eng. Tech. Res.* 6, 71 (2016).
- [37] Varshni, Y. P. Temperature dependence of the energy gap in semiconductors. *Physica* 34, 149–154 (1967).
- [38] Alam, I. & Ashraf, A. Effect of Different Device Parameters on Tin Based Perovskite Solar Cell Coupled with In₂S₃ Electron Transport Layer and CuSCN and Spiro-OMeTAD Alternative Hole Transport Layers for High Efficiency Performance Effect of Different Device Parameters on T. *Energy Sources, Part A Recover. Util. Environ. Eff.* 159, 1–17 (2020).
- [39] Priyanka Singh, N. M. R. temperature.pdf. *Sol. Energy Mater. Sol. Cells* 101, 36–45 (2012).
- [40] Abdelfatah, M. *et al.* Solar Energy Materials and Solar Cells Fabrication and characterization of low cost Cu₂O/ZnO:Al solar cells for sustainable photovoltaics with earth abundant materials. *Sol. Energy Mater. Sol. Cells* 145, 454–461 (2016).
- [41] Minemoto, Takashi, M. M. Impact of work function of back contact of perovskite solar cells without hole transport material analyzed by device simulation. *Curr. Appl. Phys.* 14, 1428–1433 (2014).
- [42] Dibyajyoti Saikia, Jayanta Bera, Atanu Betal, S. S. Performance evaluation of an all inorganic CsGeI₃ based perovskite solar cell by numerical simulation.pdf. *Opt. Mater. (Amst)*. 123, 111839 (2022).
- [43] Amir Farzaneh, Maysam Mohammadi, Z. A. and I. A. Aluminium Alloys in Solar Power – Benefits and Limitations. in *Aluminium Alloys - New Trends in Fabrication and Applications* (2012). <https://doi.org/10.5772/54721>
- [44] Ameer, K., Mazari, H. & Benseddik, N. Optimization of a GaAsN Ternary Alloy Based Solar Cell for High Efficiency. *J. New Technol. Mater.* 8, 114–119 (2018).